

Confined semiflexible polymer chains

Jörg Hendricks,¹ Toshihiro Kawakatsu,^{2,3} Kyozi Kawasaki,^{2,1} and Walter Zimmermann^{1,*}
¹*Institut für Festkörperforschung, Forschungszentrum Jülich, D-52425 Jülich, Federal Republic of Germany*
²*Department of Physics, Kyushu University 33, Fukuoka 812, Japan*
³*Department of Physics, Tokyo Metropolitan University, Hachioji, Tokyo 192-03, Japan*
 (Received 16 March 1994; revised manuscript received 11 October 1994)

Motivated by recent experiments on actin filaments, the behavior of semiflexible polymers confined between two rigid walls is investigated as a function of the wall distance. For fixed bending stiffness the persistence length depends on the wall distance and shows an interesting crossover.

PACS number(s): 61.41.+e, 87.10.+e, 36.20.-r

Actin filaments are important constituents of biological organisms and they are rather stiff. In some respects they behave as semiflexible polymers, with a persistence length of the order of the chain length. Recently, freely flickering actin filaments have been investigated in two independent experiments [1,2], where the actin filaments were confined between two walls. In both experiments different wall distances and different methods for the determination of the persistence length were used and different values for the persistence length and the bending stiffness were measured.

Here, we consider a semiflexible polymer confined between two rigid walls and we investigate its static and dynamic properties as a function of the wall distance. Special emphasis is placed on the cases where the wall distance is of the order of the persistence length and the chain length. Keeping all chain properties fixed and changing the wall distance, a crossover of the persistence length from its value in three dimensions to its value in two dimensions will be found. This crossover might be one of the possible reasons for the different experimental results.

Single semiflexible polymer chains of length $\bar{l}N$ are considered and the chain configuration is described by a vector function \mathbf{c}_s , with the contour variable s varying continuously between 0 and N . We describe the semiflexible polymer chain by a generalized Rouse model which provides in its continuum formulation the following equation of motion for \mathbf{c}_s [3]:

$$\zeta_0 \dot{\mathbf{c}}_s = -\frac{\delta}{\delta \mathbf{c}_s} H\{\mathbf{c}\} + \mathbf{f}_s. \quad (1)$$

Herein the thermal noise \mathbf{f}_s is related via the fluctuation dissipation theorem

$$\langle \mathbf{f}_s(t) \otimes \mathbf{f}_{s'}(t') \rangle = 2k_B T \zeta_0 \mathbf{1} \delta(s - s') \delta(t - t') \quad (2)$$

to the friction constant for each chain segment ζ_0 , where \otimes is the dyadic product and $\mathbf{1}$ the unit matrix. The Hamiltonian of our semiflexible chain up to the second nonvanishing order is described by [3]

$$H\{\mathbf{c}\} = \int_0^N ds \left[\frac{3k_B T}{2\bar{l}^2} \left(\frac{\partial \mathbf{c}_s}{\partial s} \right)^2 + \frac{\bar{\kappa}}{2} \left(\frac{\partial^2 \mathbf{c}_s}{\partial s^2} \right)^2 + \dots \right]. \quad (3)$$

k_B is the Boltzmann constant, T the absolute temperature, and $\bar{\kappa}$ describes the bending rigidity of the chain. Note, if $\bar{\kappa}$ vanishes, then Eq. (3) reduces to the Hamiltonian for a Gaussian chain and the length element \bar{l} may be interpreted as the Kuhn length. For finite values of $\bar{\kappa}$, the persistence length of the chain orientation, l_p , and therefore the Kuhn length, is larger than \bar{l} . A length constraint for the polymer chains provides a relation between \bar{l} and $\bar{\kappa}$. In this case the Hamiltonian given in Eq. (3) contains only one independent parameter [3,4].

For reasons described in Ref. [5], we actually simulate the chain including the inertial term $m\dot{\mathbf{c}}_s$ instead of the purely dissipative equation of motion, Eq. (1). The introduction of the inertial term is necessary to avoid a remarkable accumulation of the numerical error in the integration scheme. Additionally, we adopt a discrete description of the chain, where the chain is described by a one-dimensional string of beads connected by springs. The spring connecting neighboring monomers is assumed to have the following potential [6]:

$$H_{\text{bond}} \equiv H_{\text{LJ}} + H_{\text{FENE}}. \quad (4)$$

The first part is a purely repulsive Lennard-Jones potential,

$$H_{\text{LJ}} \equiv \begin{cases} 4\epsilon \left[\left(\frac{\sigma}{r_{ij}} \right)^{12} - \left(\frac{\sigma}{r_{ij}} \right)^6 + \frac{1}{4} \right], & r_{ij} \leq 2^{1/6} \sigma, \\ 0, & r_{ij} > 2^{1/6} \sigma, \end{cases} \quad (5)$$

and the second part is a nonlinear FENE (finite extendable nonlinear elastic) potential

$$H_{\text{FENE}} \equiv \begin{cases} -\frac{1}{2} k R_0^2 \ln \left[1 - \left(\frac{r_{ij}}{R_0} \right)^2 \right], & r_{ij} \leq R_0, \\ \infty, & r_{ij} > R_0. \end{cases} \quad (6)$$

In order to introduce the bending rigidity of the chain, i.e., the second term on the right-hand side of Eq. (3), we assume the additional potential

* Author to whom correspondence should be addressed.

$$V(\Theta_i) = -2\kappa \ln\left[\frac{1}{2}(1 + \cos \Theta_i)\right]. \quad (7)$$

Θ_i is the angle between the two neighboring bond vectors \mathbf{b}_i and \mathbf{b}_{i+1} meeting at the i th monomer, whereby the bond vector \mathbf{b}_i is defined by

$$\mathbf{b}_i = \frac{\mathbf{c}_i - \mathbf{c}_{i-1}}{|\mathbf{c}_i - \mathbf{c}_{i-1}|}, \quad (8)$$

\mathbf{c}_i being the position vector of the i th monomer and κ the bending rigidity modulus. Here it should be mentioned that there is no restoring force for the bond rotation at a finite angle φ along the azimuthal direction. Due to this bending elasticity, the statistics of the chain is not Gaussian on length scales below the persistence length. However, the large scale statistics still retains the Gaussian nature.

With those potentials and the inertial term we finally simulate the spatially discretized equations:

$$m \ddot{\mathbf{c}}_i = -\frac{\partial H}{\partial \mathbf{c}_i} - \zeta_0 \dot{\mathbf{c}}_i + \mathbf{f}_i(t), \quad (9)$$

$$\langle \mathbf{f}_i(t) \otimes \mathbf{f}_j(t') \rangle = 2\zeta_0 k_B T \delta(t - t') \delta_{ij}. \quad (10)$$

Details are described in Ref. [5].

Here, we should note that such a bond-bead model defined by the potentials given in Eq. (4) and in Eq. (7) reproduces our original Hamiltonian given in Eq. (3), if we take a continuum limit of the chain with a sufficiently strong spring and a bending modulus which guarantees a smooth contour of the chain.

The walls are located at $z = 0$ and $z = d$ and both are parallel to the x - y plane. They are assumed to be hard walls, where the monomers are elastically scattered when they meet the boundaries. On the simulation procedures, we follow the techniques described in Refs. [5] and [6]. The parameters of the model equation are optimized for our purposes, where we follow Ref. [6] for the bond potential and choose the parameters in the Lennard-Jones potential as $\sigma = 1.0$ and $\varepsilon = 1.0$. For the mass we choose $m = 1.0$ which leads to the typical time scale related to the Lennard-Jones potential $\tau = \sigma(m/\varepsilon)^{1/2} = 1.0$. The parameters of the attractive potential H_{FENE} are chosen as $k = 30.0\varepsilon/\sigma^2$ and $R_0 = 1.5\sigma$. For those parameters the minimum of the bond potential lies at $b = 0.961\sigma$. For the temperature $k_B T = 1.0\varepsilon$ is chosen and with the friction constant $\zeta_0 = 0.5(\tau m)^{-1}$ a reasonable coupling to the heat bath is obtained via the fluctuation dissipation relation and therefore no temperature drifts take place during the simulation.

Important static properties of a semiflexible polymer are its persistence length l_p and the correlation of the bond orientations $\langle \mathbf{b}_i \cdot \mathbf{b}_j \rangle$. The latter decays exponentially for the above described Hamiltonian as $\langle \mathbf{b}_i \cdot \mathbf{b}_j \rangle = \exp(-|i - j|\bar{l}/l_p)$. When the bond correlation function $\langle \mathbf{b}_i \cdot \mathbf{b}_j \rangle$ of the polymer chain is calculated in the presence of the two walls, we find by our simulations the following three typical behaviors as shown in Fig. 1 for a chain of length $49\bar{l}$, a bending elasticity $\kappa = 50\varepsilon$, and a wall distance $d = 8\bar{l}$. The bond correlation $\langle \mathbf{b}_i \cdot \mathbf{b}_j \rangle$

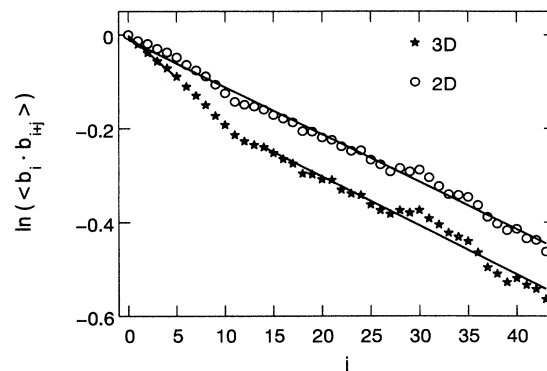


FIG. 1. The angle correlation $\ln(\langle \mathbf{b}_i \cdot \mathbf{b}_j \rangle)$ of a semiflexible polymer between two walls in three-dimensions (lower curve) and for the chain projected onto the plane of the walls (upper curve). In the angle correlation in three-dimensions there is a crossover around $|i - j|\bar{l} \sim d$ from the three dimensional behavior into the slope of that of the two-dimensional projection.

(lower curve in Fig. 1) decays exponentially and faster at short distances ($|i - j|\bar{l} < d$) than at larger distances ($|i - j|\bar{l} > d$). The crossover in the decay of $\langle \mathbf{b}_i \cdot \mathbf{b}_j \rangle$ and therefore for the corresponding persistence length happens around $|i - j|\bar{l} \propto d$. The upper curve in Fig. 1 corresponds to the bond correlation calculated from the projection of the chain onto the x - y plane. The decay length of the orientation correlation of the chain at larger distances ($|i - j|\bar{l} > d$) is similar to that of the projection onto the x - y plane. There is obviously a transition of the semiflexible polymer chain from the three-dimensional to its two-dimensional behavior, depending on the wall distance. This phenomenon holds also for other distances d and other values for the bending stiffness.

In Fig. 2 the three persistence lengths, all determined from the exponential decay of the bond correlation are plotted (a) from the initial decay at short length scales

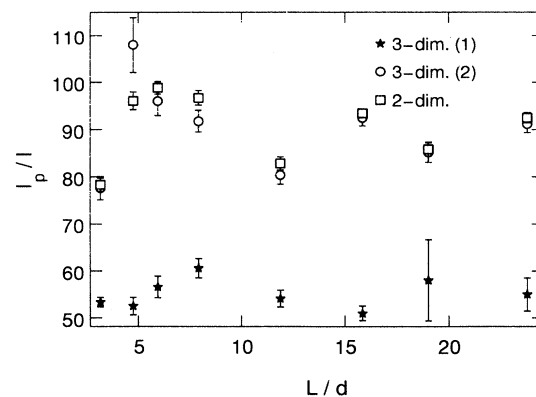


FIG. 2. The persistence length l_p determined from the three different exponential decay regimes of the bond correlation of a semiflexible polymer between two rigid walls (see Fig. 1): (\star) l_p determined from initial slope of the bond correlation, (\circ) l_p from the slope at large length scales, and (\square) l_p from the decay of the bond correlation of the chain projected into the plane of the walls.

(\star), (b) from the decay at larger length scales (\circ), and (c) from the decay along the projection of the chain into the x - y plane (\square). The persistence lengths determined from the projection and those at larger length scales agree fairly well. That means that a confined chain behaves like a two-dimensional chain at length scales larger than the wall distance d . The ratio between the persistence length for the projected conformation and that at short length scales varies roughly between 1.6 and 2, depending on the wall distance d .

On the other hand, the persistence lengths in two and

$$\langle \cos \Theta \rangle = \int_0^\pi \sin^{n-2} \Theta \cos \Theta \left[\frac{1}{2} (1 + \cos \Theta) \right]^{\frac{2\kappa}{k_B T}} d\Theta / \int_0^\pi \sin^{n-2} \Theta \left[\frac{1}{2} (1 + \cos \Theta) \right]^{\frac{2\kappa}{k_B T}} d\Theta. \quad (12)$$

Θ describes the angle between neighboring bonds:

$$\langle \mathbf{b}_i \cdot \mathbf{b}_{i+1} \rangle = \langle \cos \Theta_i \rangle. \quad (13)$$

In three dimensions one can perform the above integrals explicitly and one has

$$\langle \cos \Theta \rangle = \frac{\kappa}{\kappa + k_B T}, \quad (14)$$

whereas in two dimensions we have calculated the integrals numerically. For small values of \bar{l}/l_p one can determine the persistence length l_p by expanding $\langle \mathbf{b}_i \cdot \mathbf{b}_{i+1} \rangle = \exp(-\bar{l}/l_p)$:

$$l_p = \frac{\bar{l}}{1 - \langle \cos \Theta \rangle}. \quad (15)$$

This provides also the analytical relation between the persistence length l_p and the bending elasticity κ in three dimensions, $l_p = \bar{l}(1 + \kappa/k_B T)$. In two dimensions the analytical relation between l_p and κ is more complex. The persistence length $l_p(\kappa)$ as a function of κ , determined from the simulations via the orientational correlation shown in Fig. 1, is in good agreement with the analytical relations given above (described in more detail in Ref. [5]). The persistence lengths l_{p2} and l_{p3} , in

three spatial dimensions can be calculated semianalytically for discrete chains of fixed bond length, as explained in the following. For the bending potential given in Eq. (7) one can calculate via

$$\langle \cos \Theta \rangle = \frac{\int d\Omega \cos \Theta e^{-V(\Theta)/k_B T}}{\int d\Omega e^{-V(\Theta)/k_B T}} \quad (11)$$

the angle distribution in two ($n = 2$) and three ($n = 3$) spatial dimensions, with $d\Omega = d\Theta$ and $d\Omega = 2\pi \sin \Theta d\Theta$, respectively:

two and three spatial dimensions, respectively, can be calculated via Eq. (15), whereas $\langle \cos \Theta \rangle$ from Eq. (12) must be numerically evaluated for $n = 2$. The ratio between the two persistence lengths l_{p2} and l_{p3} is plotted in Fig. 3 as a function of the bending stiffness κ . The ratio starts at the value 1 and increases to its limiting value 2, where the persistence lengths in two and three dimensions both diverge. The different values for l_{p2} and l_{p3} at the same value of the bending stiffness have their origin in the constraint of fixed chain length. Without that constraint the persistence lengths are the same in two and three spatial dimensions [5]. In our numerical simulation the chain length is not rigidly fixed; therefore the ratios for l_{p3}/l_{p2} in Fig. 2 are smaller than 2 and vary between 1.6 and 2.0.

Another static quantity for a polymer chain, the mean-squared end-to-end distance $\langle R^2 \rangle = \langle (\mathbf{c}_1 - \mathbf{c}_N)^2 \rangle$ increases with decreasing wall distance d from the three-dimensional bulk value to its two-dimensional one. In the absence of the walls, the persistence length calculated from numerical results for the end-to-end distance via the analytical relation [3,7]

$$\langle R^2 \rangle = 2l_p^2 \left(\frac{L}{l_p} - 1 + e^{-L/l_p} \right) \quad (16)$$

is in good agreement with the value for the persistence length determined from the bond correlation. However, for polymers confined between two rigid walls [5] [with $L = \bar{l}(N - 1)$], the two approaches usually give different values, especially in the range $L > d > l_p$. This has to be taken into account when persistence lengths determined by different methods are compared.

A further possible way for characterizing the static properties of a polymer is the decomposition of the polymer contour into normal modes, the so-called Rouse modes,

$$\mathbf{X}_p = \frac{1}{N} \sum_{i=1}^N \mathbf{c}_i(t) \cos \left[\frac{p\pi(i-1)}{N-1} \right], \quad (17)$$

where $p = 0, 1, \dots, N-1$. Similarly to the static structure factor, the Rouse modes also provide information about the internal structure of the polymer. Starting with the potential in the continuum limit in Eq.(3), it is easy to

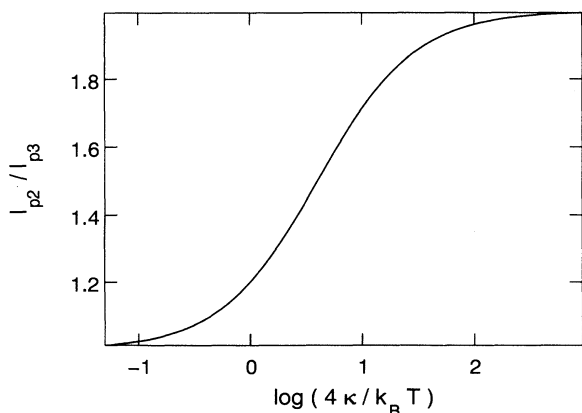


FIG. 3. The ratio of the persistence length l_{p2} in two dimensions and in three dimensions l_{p3} calculated from Eq. (12) as a function of the normalized bending elasticity $4\kappa/k_B T$.

calculate

$$\langle \mathbf{X}_p^2 \rangle = \frac{3k_B T}{[3k_B T/\bar{l}^2]q^2 + \bar{\kappa}q^4}, \quad (18)$$

with $q = \pi p/N$. This reduces in the case of an ideal random walk, $\bar{\kappa} = 0$, to the well known scaling relation $\langle \mathbf{X}_p^2 \rangle \propto 1/p^2$. In the experiment described in Ref. [1], the slope of the actin contour was measured and decomposed in its Fourier modes and from the measured data a quantity proportional to $(q^4 \langle \mathbf{X}_p^2 \rangle)^{-1} = \frac{1}{3k_B T} [\frac{3k_B T}{\bar{l}^2 q^2} + \bar{\kappa}]$ has been extracted, which becomes for large values of q ($p \sim N$) proportional to the constant $\bar{\kappa}$. This expression for $\langle \mathbf{X}_p^2 \rangle$ obviously shows a crossover near $q^2 = 3k_B T \bar{\kappa} / \bar{l}^2$, at length scales of the order of the persistence length, where a transition occurs from the rigid rod regime at short lengths to the Gaussian chain regime for flexible polymers at larger length scales. The experimental measurements on actin in Ref. [1] detect a crossover too, which finds its natural interpretation in the above-mentioned mode spectrum calculation of the semiflexible polymer chains.

In Ref. [2] an exponential decay of the bond correlation was measured, which the authors insisted to be incompatible with a wave number dependent apparent bending stiffness as measured in Ref. [1]. However, a wave number dependent behavior of $(p^4 \langle \mathbf{X}_p^2 \rangle)^{-1}$, is not in contradiction with exponential decay for the orientational correlation along the chain (see also [4,5]). As the persistence length observed in Ref. [2] is rather large ($l_p > 0.5L$), it might be difficult to detect a crossover in the quantity $(p^4 \langle \mathbf{X}_p^2 \rangle)^{-1}$ in this experiment, contrary to the case in Ref. [1].

There are at least three possible reasons why a smaller value for the persistence was reported in Ref. [1] than in Ref. [2]. (1) The confinement of the actin to two dimensions, as in Ref. [2], might lead to a larger persistence length as explained in this note. (2) A further possible origin for the different persistence lengths is the defects in the actin filament described in Ref. [1]. Such defects lead to larger mode amplitudes $|X_p|$ and therefore to an apparently lower bending modulus as well as to a

smaller persistence length. (3) Also, different experimental methods might be a possible reason for the different values of the persistence length l_p . Ott *et al.* determined the persistence length l_p from the decay of the orientational correlation of the measured contour. The decay length of the orientational correlation is a rather natural definition of the persistence length l_p . Käs *et al.* determined l_p indirectly by measuring first the spectrum X_p and calculating from that spectrum the bending elasticity $\bar{\kappa}$. Finally, they calculated l_p from the bending elasticity $\bar{\kappa}$ via a simple formula.

We did some consistency tests for our simulations. In one case, for various input values of κ the persistence lengths $l_p(\kappa)$ have been determined from the orientational correlation in the simulations and from those values of $l_p(\kappa)$ we calculated κ via the expression $\kappa = k_B T (l_p/\bar{l} - 1)$, and compared it with the input value for κ . There is good agreement between the κ values determined in this way from the simulations and the input values. A similar consistency test for the radius of gyration was also satisfying (for details, we refer to Ref. [5]). From that point of view the determination of l_p from the orientational correlation was rather robust. [κ determined by fitting the ansatz given in Eq. (18) to the mode spectrum obtained from the simulations is in less good agreement with the input value of κ ; the actual value of κ is underestimated.] In that respect it would be desirable for the persistence length l_p to be determined from both sets of experimental data from the orientational correlation. That would allow one to sort out whether the different values for l_p found in the experiments described in Refs. [1,2] have their origin in the different determination procedure or whether the difference is characteristic for the materials used.

W.Z. would like to thank H. Strey and A. Libchaber for useful information and K. Kremer for instructive discussions. K.K. would like to thank the Humboldt Foundation for support that made his stays in Jülich possible. T.K. thanks Yamada Science Foundation and the KFA Jülich for financial support and W.Z. the Kajima Foundation.

-
- [1] J. Käs, H. Strey, M. Bärmann, and E. Sackmann, *Europhys. Lett.* **21**, 865 (1993).
 [2] A. Ott, M. Magnasco, A. Simon, and A. Libchaber, *Phys. Rev. E* **48**, R1642 (1993).
 [3] R. Harris and J. Hearst, *J. Chem. Phys.* **44**, 2595 (1966).
 [4] J. Lagowski, J. Noolandi, and B. Nickel, *J. Chem. Phys.*

- 95**, 1266 (1991).
 [5] J. Hendricks, T. Kawakatsu, K. Kawasaki, and W. Zimmermann (unpublished).
 [6] G. Grest and K. Kremer, *Phys. Rev. A* **33**, 3628 (1986).
 [7] M. Doi and S.F. Edwards, *The Theory of Polymer Dynamics* (Clarendon Press, Oxford, 1986).